



## The stability of a static liquid column pulled out of an infinite pool

E. S. Benilov<sup>a)</sup> and C. P. Cummins<sup>b)</sup>

*Department of Mathematics, University of Limerick, Limerick, Ireland*

(Received 29 May 2013; accepted 20 October 2013; published online 7 November 2013)

We study the stability of a static liquid column rising from an infinite pool, with its top attached to a horizontal plate suspended at a certain height above the pool's surface. Two different models are employed for the column's contact line. Model 1 assumes that the contact angle always equals Young's equilibrium value. Model 2 assumes a functional dependence between the contact angle and the velocity of the contact line, and we argue that, if this dependence involves a hysteresis interval, linear perturbations cannot move the contact line. It is shown that, within the framework of Model 1, all liquid columns are unstable. In Model 2, both stable and unstable columns exist (the former have larger contact angles  $\theta$  and/or larger heights  $H$ ). For Model 2, the marginal stability curve on the  $(\theta, H)$ -plane is computed. The mathematical results obtained imply that, if the plate to which a stable liquid column is attached is slowly lifted up, the column's contact line remains pinned while the contact angle is decreasing. Once it reaches the lower boundary of the hysteresis interval, the column breaks down. © 2013 AIP Publishing LLC. [<http://dx.doi.org/10.1063/1.4829275>]

### I. INTRODUCTION

If a disk made of a wettable material is dipped in an infinite pool of liquid and then slowly lifted up, a liquid column with its top attached to the disk is pulled out of the pool (see Fig. 1). If the disk keeps being lifted up, one would expect the column to reach a certain threshold height and break down.

There have been two attempts to explain the breakdown of liquid columns. In Ref. 1, it was argued that, unless the liquid covers the entire disk, the column is unstable, which suggests the following scenario: immediately after the dipping, and up to a certain height, the disk is indeed entirely covered with liquid – but then the column begins to contract and, once its top retreats from the disk's edge, the loss of stability causes a break-down.

Reference 2, on the other hand, suggested that the break-down can be explained by non-existence of a solution for a static column with its height exceeding a certain critical value. Reference 2 also presented an incomplete stability analysis (involving a certain class of perturbations) and showed that at least some of the columns with less-than-critical heights are unstable.

The present work stems from a simple experiment, the result of which is presented in Fig. 1: one can see an evidently stable column with its top *not* covering the entire disk. Given that the analysis of Ref. 1 is verifiably correct, the discrepancy between the theoretical and experimental results can only be clarified by re-examining the problem's physical foundations.

In this work, we demonstrate that the stability of a liquid column depends strongly on the dynamics of the contact line (i.e., the curve of intersection of the disk and the liquid/gas interface). Two different models of contact lines will be discussed, assuming the disturbances to preserve either (1) the contact angle or (2) the contact line's position. Model 1 has been widely used in stability studies of capillary surfaces (including Refs. 1 and 2). Model 2, in turn, has been used only in

<sup>a)</sup>Electronic mail: [Eugene.Benilov@ul.ie](mailto:Eugene.Benilov@ul.ie). URL: <http://www.staff.ul.ie/eugenebenilov/hpage/>.

<sup>b)</sup>Electronic mail: [Cathal.Cummins@ul.ie](mailto:Cathal.Cummins@ul.ie). URL: [http://www.macs.ul.ie/person.php?key=cummins\\_cathal](http://www.macs.ul.ie/person.php?key=cummins_cathal).

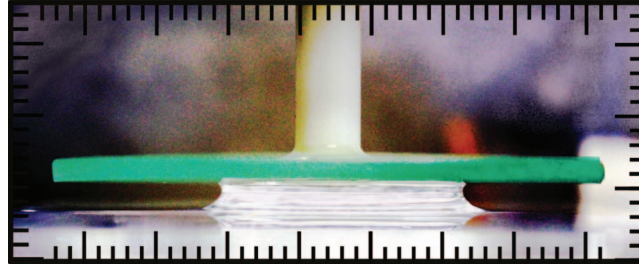


FIG. 1. An example of a liquid column with its top attached to a solid disk (de-ionized water and polished glass, respectively). The column's dimensions can be estimated using the rulers at the edges of the figure (the spacing between large ticks is 1 cm).

Ref. 3, where it was shown to follow from the existence of a hysteresis interval in the dependence of the contact line's velocity on the contact angle. It turns out that Model 2 does describe stable columns with their tops *not* covering the entire disk.

This paper has the following structure: in Secs. II and III, we formulate the energy minimization problem describing the stability of liquid columns attached to a horizontal disk and, in Secs. IV and V, present its solution. In Sec. VI, we shall compare our results to those of Refs. 1 and 2.

## II. FORMULATION

Consider a horizontal plate (approximating the disk) suspended above an infinite pool of an incompressible liquid of density  $\rho$ , and a liquid column rising from the pool, with its top attached to the plate (see Fig. 2). Let the liquid/gas, gas/solid, and solid/liquid interfaces be characterized by the capillary coefficients  $\sigma_{lg}$ ,  $\sigma_{gs}$ , and  $\sigma_{sl}$ , respectively. We also introduce the acceleration due to gravity  $g$ , the liquid/gas capillary scale,

$$L = \sqrt{\frac{\sigma_{lg}}{\rho g}},$$

and Young's equilibrium angle

$$\theta = \arccos \frac{\sigma_{gs} - \sigma_{sl}}{\sigma_{lg}}, \quad (1)$$

which is, essentially, the value of the contact angle (between the liquid/gas and solid/liquid interfaces) for which the contact line is in static equilibrium.

In terms of cylindrical coordinates, the surface of the column is determined by

$$r = r(\phi, z),$$

where  $\phi$ ,  $z$ , and  $r$  are the polar angle, and the axial and radial coordinates, respectively. It is implied that  $r$  and  $z$  are non-dimensionalized by  $L$ , and the plane  $z = 0$  corresponds to the pool's unperturbed surface.

We shall adopt the variational approach to stability, according to which a steady state  $r(\phi, z)$  is stable with respect to small (linear) perturbations, if a functional  $E[r]$  exists such that, for this steady state,  $\delta E = 0$  and  $E$  has a local minimum. It can be shown (e.g., Ref. 4) that these conditions hold if

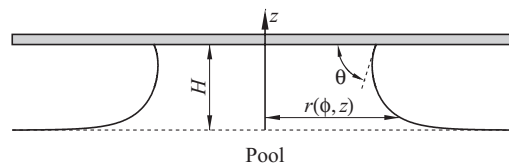


FIG. 2. A capillary surface  $r = r(z, \phi)$  rising from an infinite pool and attached to a horizontal plate located at a height  $H$ .  $\theta$  is the contact angle (between the plate and the capillary surface).

$\delta^2 E$  is *strongly positive*, i.e.,

$$\delta^2 E \geq \mu \|\delta r\|^2, \quad (2)$$

where  $\mu > 0$ . In what follows, we shall use the following norm:

$$\|f\| = \left[ \int_0^\infty \int_0^{2\pi} f^2(\phi, z) r \, d\phi \, dr \right]^{1/2}. \quad (3)$$

Note that, in physical literature on stability (originating from Ref. 5), condition (2) is often replaced with the weaker requirement  $\delta^2 E > 0$  – which, however, does *not* guarantee that  $E$  has a minimum (see Scheeffer's counter-example on page 266 in Ref. 6).

In most cases,  $E$  is the energy of the system, and depending on the specifics of the problem, the first and second variations of  $E$  should be calculated under additional constraints, such as conservation of mass, etc.

### A. The energy functional

Denoting the (non-dimensional) height of the plate by  $H$ , we introduce the (non-dimensional) energy as

$$E = P + S_{gs} + S_{sl} + S_{lg}, \quad (4)$$

where

$$P = \int_0^{2\pi} \int_0^H \frac{z r^2}{2} \, dz \, d\phi \quad (5)$$

is the potential energy of gravity, and  $S_{lg}$ ,  $S_{gs}$ , and  $S_{sl}$  represent the surface energy of the liquid/gas, gas/solid, and solid/liquid interfaces, respectively. To avoid the divergency associated with the plate's surface being infinite, let  $S_{gs}$  represent the energy difference between the current (partially wet) and initial (all dry) states. It is also convenient to combine  $S_{gs}$  with  $S_{sl}$ , which yields

$$S_{gs} + S_{sl} = -\cos \theta \int_0^{2\pi} \frac{(r^2)_{z=H}}{2} \, d\phi. \quad (6)$$

To avoid the divergency resulting from the liquid/gas interface being infinite, we first truncate the column at  $z = z_0 > 0$  and calculate its surface energy, then subtract the energy of a flat region enclosed by the curve  $r = r(\phi, z_0)$  (which would be in place of the truncated column if the liquid was unperturbed). Eventually we take the limit  $z_0 \rightarrow 0$ , which yields

$$S_{lg} = \lim_{z_0 \rightarrow 0} \int_0^{2\pi} \left[ \int_{z_0}^H \sqrt{1 + \left( \frac{1}{r} \frac{\partial r}{\partial \phi} \right)^2 + \left( \frac{\partial r}{\partial z} \right)^2} r \, dz - \left( \frac{r^2}{2} \right) \right] d\phi. \quad (7)$$

Expressions (4)–(7) determine  $E$  in terms of  $r(\phi, z)$ .

### B. Volume conservation

Before varying  $E$ , observe that, if the pool under consideration was finite, the allowable perturbations would have to satisfy the condition of volume (mass) conservation. This condition can be formulated as a requirement that the volume  $V$  of the liquid above the level  $z = 0$  be constant – this way,  $V$  remains finite even if the pool is infinite,

$$V = \int_0^{2\pi} \int_0^H \frac{r^2}{2} \, dz \, d\phi. \quad (8)$$

Treating the infinite pool as a limit of increasingly large, but finite ones, and keeping in mind that perturbations in the latter must preserve volume, we require the same for the former. Thus, the variation  $\delta r$  should satisfy the condition  $\delta V = 0$ .

Note that Ref. 1 did *not* impose the constraint of volume conservation.

### C. The dynamics of the contact line

It turns out that the column's stability depends strongly on the dynamics of the contact line. We shall carry out the analysis for two commonly used models, originating from Refs. 7 and 8 – which will be referred to as Models 1 and 2, respectively.

Model 1 requires the contact angle to always equal  $\theta$  [defined by (1)]. Model 2, in turn, assumes a functional dependence between the contact angle and the contact-line's velocity. Most importantly, this dependence almost always involves a hysteresis interval, i.e., a range of contact angles  $(\theta_r, \theta_a)$  for which the contact line is stationary. It can advance or recede only if the contact angle is greater than  $\theta_a$  or less than  $\theta_r$ , respectively.

As noted in Ref. 3, Model 2 has important implications for the linear stability of a steady state with a contact line. Since the contact line is stationary, the contact angle must either equal  $\theta_r$  or  $\theta_a$ , or be inside the hysteresis interval. The latter is more probable, of course – hence, we assume the contact angle of a steady state to be separated from both  $\theta_r$  and  $\theta_a$  by *finite* gaps. This effectively means that a linear (*infinitesimally small*) perturbation cannot move the contact line.

Thus, when examining linear stability of a steady state involving a liquid/solid/gas combination with a hysteresis interval, one can safely assume the contact line to be pinned to the solid.

One can arrive at the same conclusion through the following qualitative argument: consider a drop on a plate which is being shaken by external force. Our everyday experience suggests that, if the liquid is not perfectly wetting and the plate's oscillations are sufficiently weak, the drop would remain in its original position. The same should hold if the external force is replaced by a sufficiently weak internal (self-generated) perturbation – and, finally, if the drop is replaced with a liquid column.

Thus, we summarize

- Model 1 assumes the *contact angle* to be fixed. It will be later shown that this requirement does not need to be specifically imposed as it follows naturally from the condition  $\delta E = 0$ .
- Model 2 assumes the contact line's *position* to be fixed. In this case we need to specifically require

$$r = R(\phi) \quad \text{at} \quad z = H, \quad (9)$$

where  $R(\phi)$  is a given function. In the context of our variational problem, condition (9) is a “holonomic constraint.”

Reference 1 did not explicitly assume either of the above models, but the perturbations considered did preserve the contact angle.

Reference 1 also argued that, if the column's top covers the entire disk, the contact line gets pinned to the disk's edge, and the column can become stable. We shall return to this issue later in Sec. VI.

## III. THE VARIATIONAL PROBLEM

### A. The first variation of $E$

Varying the functional  $E$  [given by (4)–(7)], one obtains

$$\delta E = \int_0^{2\pi} \int_0^H z r \delta r \, dz \, d\phi - \cos \theta \int_0^{2\pi} (r \delta r)_{z=H} \, d\phi + \delta S_{lg} \quad (10)$$

where

$$\delta S_{lg} = \lim_{z_0 \rightarrow 0} \int_0^{2\pi} \left\{ \int_{z_0}^H \left[ \frac{-\frac{\delta r}{r^2} \left( \frac{\partial r}{\partial \phi} \right)^2 + \frac{1}{r} \frac{\partial r}{\partial \phi} \frac{\partial \delta r}{\partial \phi} + r \frac{\partial r}{\partial z} \frac{\partial \delta r}{\partial z}}{\sqrt{\Delta}} + \sqrt{\Delta} \delta r \right] dz - (r \delta r)_{z=z_0} \right\} d\phi \quad (11)$$

and

$$\Delta = 1 + \left( \frac{1}{r} \frac{\partial r}{\partial \phi} \right)^2 + \left( \frac{\partial r}{\partial z} \right)^2.$$

Expression (11) can be re-arranged by “isolating” the terms involving  $\partial \delta r / \partial \phi$  and  $\partial \delta r / \partial z$  and integrating them by parts with respect to  $\phi$  and  $z$ , respectively. Then, (10) becomes

$$\begin{aligned} \delta E = \lim_{z_0 \rightarrow 0} \int_0^{2\pi} \left\{ \int_{z_0}^H \left[ \frac{1 + \left( \frac{\partial r}{\partial z} \right)^2}{\sqrt{\Delta}} - \frac{\partial}{\partial \phi} \frac{1}{r} \frac{\partial r}{\partial \phi} - \frac{\partial}{\partial z} \frac{r}{\sqrt{\Delta}} \frac{\partial r}{\partial z} + zr \right] \delta r dz + \left( r + \frac{r}{\sqrt{\Delta}} \frac{\partial r}{\partial z} \right)_{z=z_0} (\delta r)_{z=z_0} \right\} d\phi \\ + \int_0^{2\pi} \left( \frac{r}{\sqrt{\Delta}} \frac{\partial r}{\partial z} - r \cos \theta \right)_{z=H} (\delta r)_{z=H} d\phi. \end{aligned} \quad (12)$$

Up to this point, our analysis did not depend on the model of the contact-line dynamics, but now we should specify whether we use Model 1 or 2. For Model 1, the requirement  $\delta E = 0$  implies that, in expression (12), the coefficients of  $\delta r$ ,  $(\delta r)_{z=H}$ , and  $(\delta r)_{z=z_0}$  (in the limit  $z_0 \rightarrow 0$ ) must vanish – hence,

$$\frac{1}{r} \left[ \frac{\partial}{\partial \phi} \frac{\frac{1}{r} \frac{\partial r}{\partial \phi}}{\sqrt{1 + \left( \frac{1}{r} \frac{\partial r}{\partial \phi} \right)^2 + \left( \frac{\partial r}{\partial z} \right)^2}} + \frac{\partial}{\partial z} \frac{r \frac{\partial r}{\partial z}}{\sqrt{1 + \left( \frac{1}{r} \frac{\partial r}{\partial \phi} \right)^2 + \left( \frac{\partial r}{\partial z} \right)^2}} - \frac{1 + \left( \frac{\partial r}{\partial z} \right)^2}{\sqrt{1 + \left( \frac{1}{r} \frac{\partial r}{\partial \phi} \right)^2 + \left( \frac{\partial r}{\partial z} \right)^2}} \right] = z, \quad (13)$$

$$r + \frac{r \frac{\partial r}{\partial z}}{\sqrt{1 + \left( \frac{1}{r} \frac{\partial r}{\partial \phi} \right)^2 + \left( \frac{\partial r}{\partial z} \right)^2}} \rightarrow 0 \quad \text{as} \quad z \rightarrow 0, \quad (14)$$

$$\frac{\frac{\partial r}{\partial z}}{\sqrt{1 + \left( \frac{1}{r} \frac{\partial r}{\partial \phi} \right)^2 + \left( \frac{\partial r}{\partial z} \right)^2}} = \cos \theta \quad \text{at} \quad z = H. \quad (15)$$

Eq. (13) is the standard equation for liquid bridges,<sup>9–11</sup> equating the local curvature of a capillary surface to its height (both non-dimensional). The boundary condition (14), in turn, describes how the column’s periphery “merges” to the pool’s unperturbed level. Finally, the boundary condition (15) equates the cosine of the contact angle [the left-hand side of (15)] to the cosine of Young’s equilibrium angle  $\theta$ .

Thus, Eqs. (13)–(15) form the boundary-value problem describing our steady state (the liquid column) – and, if these equations are satisfied,  $\delta E$  is indeed zero.

For Model 2, observe that constraint (9) implies

$$\delta r = 0 \quad \text{at} \quad z = H. \quad (16)$$

This condition has no impact on the first term in expression (12), but the last term vanishes regardless of  $r$  and its derivatives. Thus, to enforce  $\delta E = 0$  for Model 2, condition (15) is not needed, and should be replaced by the holonomic constraint (9).

Thus, the Model-2 version of the boundary-value problem for  $r(\phi, z)$  consists of (13)–(14) and (9).

## B. Solutions describing liquid columns

We shall now briefly describe the solutions of the boundary-value problems (13)–(15) and (13)–(14), (9). In both cases, we are interested in axisymmetric columns, for which (13)–(15) and (9) become

$$\frac{rr'' - 1 - (r')^2}{r[1 + (r')^2]^{3/2}} = z, \quad (17)$$

$$r \rightarrow +\infty, \quad r' \rightarrow -\infty, \quad \frac{r}{(r')^2} \rightarrow 0 \quad \text{as} \quad z \rightarrow 0, \quad (18)$$

$$r' = \cot \theta \quad \text{at} \quad z = H \quad (\text{Model 1}), \quad (19)$$

$$r = R \quad \text{at} \quad z = H \quad (\text{Model 2}), \quad (20)$$

where the prime denotes differentiation with respect to  $z$ .

Solutions of (17)–(19) have been examined in Ref. 2. It was shown that, if the column's height  $H$  is increasing, its radius grows (see examples in Fig. 3). Eventually, when  $H$  reaches a threshold value of

$$H = 2 \cos \frac{1}{2}\theta, \quad (21)$$

the column becomes *infinitely* wide, and no solution exists for greater  $H$  (for more details, see Ref. 2). This property of the solution is best illustrated by the dependence of the radius  $R$  of the column's top on  $H$  (see Fig. 4).

The solutions of the Model-2 boundary-value problem (17)–(18), (20) are essentially the same as their Model-1 counterparts. The only difference is that the former are parameterized by  $(R, H)$ , whereas the latter, by  $(\theta, H)$  (as illustrated in the caption of Fig. 3). Then it can be readily deduced that (17)–(18), (20) have a solution only if  $0 < H < 2$  (where the upper bound corresponds to (21) with  $\theta = 0$ ).

Finally, we mention that

$$r = -\ln z + O(\ln |\ln z|) \quad \text{as} \quad z \rightarrow 0 \quad (22)$$

(as shown in Ref. 2).

## C. The second variation

Before calculating  $\delta^2 E$ , we need to clarify the asymptotic behavior of  $\delta r$  as  $z \rightarrow 0$ . Since  $\delta r$  represents a *small* perturbation of the steady state  $r$ , it is natural to require

$$\frac{|\delta r|}{r} \rightarrow \text{const.} \quad \text{as} \quad z \rightarrow 0, \quad (23)$$

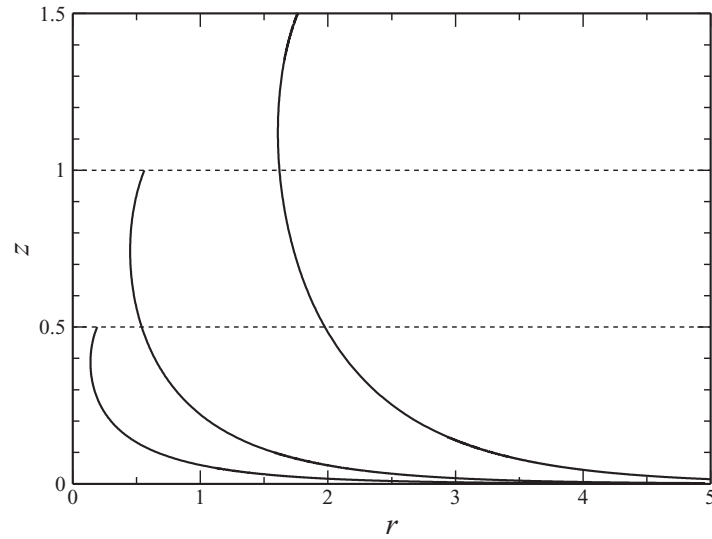


FIG. 3. Numerical solutions of the boundary-value problem (17)–(19) for Model 1 with  $H = 0.5, 1, 1.5$ , and  $\theta = 45^\circ$ . These solutions also satisfy the Model 2 boundary-value problem (17)–(18), (20) with the same values of  $H$  and  $R \approx 0.191, 0.565, 1.763$ .

where the const. is small or even zero. Note that, given asymptotic (22), it follows from (23) that

$$\frac{|\delta r|}{r'} \rightarrow 0 \quad \text{as} \quad z \rightarrow 0. \quad (24)$$

To calculate  $\delta^2 E$ , we shall vary (10). Recalling that  $r$  is axisymmetric, we integrate by parts the term involving

$$\delta r \frac{\partial \delta r}{\partial z} = \frac{\partial}{\partial z} \frac{(\delta r)^2}{2},$$

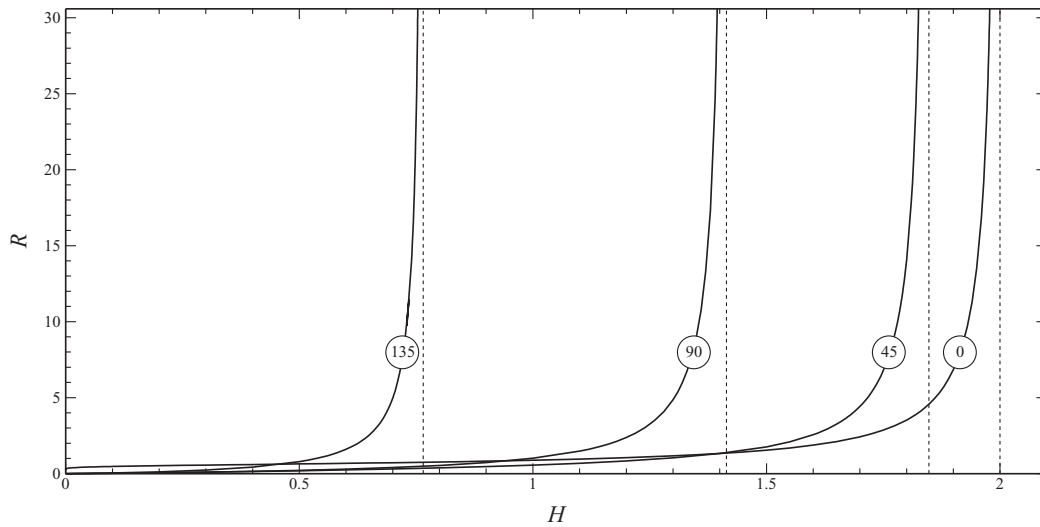


FIG. 4. The radius  $R$  of the column's top vs its height  $H$ . The curves are marked with the corresponding values of the contact angle  $\theta$ . Vertical dotted lines show the column's maximum height for the corresponding value of  $\theta$  as predicted by formula (21).

and take into account (24), which yields

$$\delta^2 E = \int_0^{2\pi} \int_0^H \frac{r^2 \left( \frac{\partial \delta r}{\partial z} \right)^2 + [1 + (r')^2] \left[ \left( \frac{\partial \delta r}{\partial \phi} \right)^2 - (\delta r)^2 \right]}{r [1 + (r')^2]^{3/2}} dz d\phi. \quad (25)$$

To prove that a column is stable, one should demonstrate that  $\delta^2 E$  is strongly positive [i.e., satisfies (2)] for all perturbations  $\delta r(\phi, z)$  that preserve the column's volume. The condition of volume preservation can be derived by varying (8) and equating  $\delta V$  to zero,

$$\int_0^{2\pi} \int_0^H r \delta r dz d\phi = 0. \quad (26)$$

Unlike the steady state  $r(z)$ , the perturbation  $\delta r(\phi, z)$  may depend on  $\phi$ . It turns out, however, that it is sufficient to examine axisymmetric perturbations.<sup>1</sup> Indeed, observe that the term involving  $\partial \delta r / \partial \phi$  in expression (25) is positive – hence,

$$\delta^2 E[\delta r(\phi, z)] \geq \delta^2 E[\bar{\delta r}(z)],$$

where

$$\bar{\delta r}(z) = \frac{1}{2\pi} \int_0^{2\pi} \delta r(\phi, z) d\phi.$$

Thus, instead of (25), it is sufficient to examine

$$\mathcal{E} = \int_0^H \frac{r^2 (f')^2 - [1 + (r')^2] f^2}{r [1 + (r')^2]^{3/2}} dz, \quad (27)$$

where

$$\mathcal{E} = \frac{\delta^2 E}{2\pi}, \quad f = \delta r,$$

and  $f$  depends only on  $z$ . The volume-preserving condition (26), in turn, becomes

$$\int_0^H r f dz = 0, \quad (28)$$

and we shall also impose a normalizing condition of the form

$$\int_0^H f^2 dz = a^2, \quad (29)$$

where the constant  $a$  can be chosen as convenient.

In addition to restrictions (28) and (29), the perturbation must satisfy (23), where  $\delta r$  is to be changed to  $f$ ,

$$\frac{|f|}{r} \rightarrow \text{const.} \quad \text{as} \quad z \rightarrow 0. \quad (30)$$

Finally, we require that the perturbation cannot change either the contact angle (Model 1) or the position of the contact line (Model 2):

$$f' = 0 \quad \text{if} \quad z = H \quad (\text{Model 1}), \quad (31)$$

$$f = 0 \quad \text{if} \quad z = H \quad (\text{Model 2}). \quad (32)$$

The variational problems (27)–(31) and (27)–(30), (32) will be examined in Sec. IV.



#### IV. THE ENERGY-MINIMIZING PERTURBATION

To examine the stability of a column described by, say, Model 1, one should minimize  $\mathcal{E}$  subject to constraints (28)–(31) and check whether its minimum value is positive (stability) or negative (instability). The simplest way to solve this variational problem consists in reducing it to a certain eigenvalue problem.<sup>11</sup>

##### A. Reduction of the variational problem to an eigenvalue problem

Observe that, if  $\mathcal{E}$  has a minimum, it must have a stationary point – i.e.,  $f$  must exist such that the first variation of  $\mathcal{E}$  is zero. Recalling that  $f$  should also satisfy the volume-preserving and normalizing conditions (28) and (29), we require

$$\delta \left[ \mathcal{E} - \lambda \int_0^H r f \, dz - \mu \left( \int_0^H f^2 \, dz - a^2 \right) \right] = 0, \quad (33)$$

where  $\lambda$  and  $\mu$  are the Lagrange multipliers. Substituting  $\mathcal{E}$  from (27) into (33) and integrating by parts the term involving  $f' \delta f'$ , we obtain

$$\left\{ \frac{r f'}{[1 + (r')^2]^{3/2}} \right\}' + \frac{f}{r [1 + (r')^2]^{1/2}} + \frac{\lambda r}{2} + \mu f = 0 \quad (34)$$

(note that the “boundary” terms resulting from the integration by parts vanish due to conditions (30)–(32) for  $f$  and similar conditions for  $\delta f$  following from those).

Together with (28)–(31) (Model 1) or (28)–(30), (32) (Model 2), Eq. (34) forms an eigenvalue problem where  $f(z)$  is the eigenfunction and  $\mu$  is the eigenvalue. The parameter  $\lambda$ , in turn, plays the role of a normalizing constant and, unless  $\lambda = 0$ , it can be eliminated by changing

$$f \rightarrow \lambda f, \quad a \rightarrow \lambda a \quad (35)$$

in Eqs. (34) and (29). We shall not do this, however, as  $\lambda$  can sometimes vanish (see below).

Once the eigenvalue problem for  $f(z)$  and  $\mu$  is solved, the former is inserted into expression (27) for  $\mathcal{E}$ , the sign of which indicates either stability ( $\mathcal{E} \geq 0$ ) or instability ( $\mathcal{E} < 0$ ).

It can be shown, however, that one does not need to calculate  $\mathcal{E}$  to find its sign, as it coincides with that of  $\mu$ . To prove this, multiply (34) by  $f$  and integrate with respect to  $z$  from 0 to  $H$ ,

$$\int_0^H \left\{ \frac{r f'}{[1 + (r')^2]^{3/2}} \right\}' f \, dz + \int_0^H \frac{f^2 \, dz}{r [1 + (r')^2]^{1/2}} + \frac{\lambda}{2} \int_0^H r f \, dz + \mu \int_0^H f^2 \, dz = 0.$$

The third term in this equality vanishes due to (28). Integrating the first term by parts and taking into account the boundary conditions for either Model 1 or 2, we obtain

$$-\mathcal{E} + \mu \int_0^H f^2 \, dz = 0. \quad (36)$$

This equality shows that  $\mathcal{E}$  and  $\mu$  have indeed the same sign.

Furthermore, equality (36) proves that, if  $\mu > 0$ , the functional  $\mathcal{E} = \delta^2 E$  is strongly positive, i.e., satisfies conditions (2) and (3). The constant  $\mu$  which appears in (2) should be identified with the eigenvalue of our eigenvalue problems for Models 1 and 2. Then, if  $\delta r$  is the minimizing disturbance, condition (2) holds as an equality – and, for all other disturbances, it holds as an *inequality*.

Even though the above eigenvalue problems for Models 1 and 2 are simpler than their variational counterparts, they still do not have obvious analytical solutions and, thus, should be solved numerically. Before choosing a numerical method, however, one has to clarify the behavior of solutions of Eq. (34) near the singular point  $z = 0$  (see Appendices A and B). The numerical method itself is described in Appendix C.

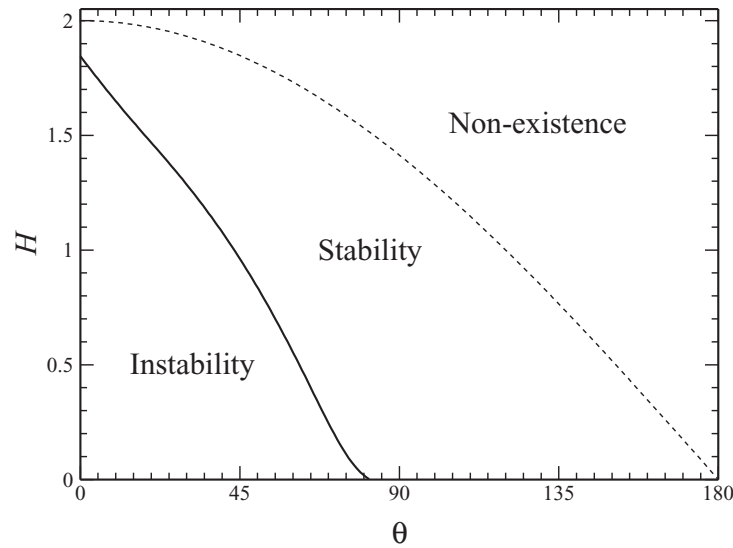


FIG. 5. The curves of neutral stability on the  $(\theta, H)$  plane for Model 2. The dotted line is the boundary of a region where no steady columns exist. For Model 1, all existing columns are unstable.

## B. The results

We shall now present the numerical results obtained for the eigenvalue problems (34), (28)–(31) (Model 1), and (34), (28)–(30), (32) (Model 2):

- (1) All columns described by Model 1 (fixed contact angle) are unstable.
- (2) Some of the columns described by Model 2 (fixed position of the contact line) are unstable, but some are stable (see the marginal stability curve<sup>12</sup> on the  $(\theta, H)$  plane in Fig. 5). In particular, columns with  $\theta \gtrsim 82^\circ$  are stable for all  $H$  and columns with  $H \gtrsim 1.85$  are stable for all  $\theta$ .

The existence of stable columns in Model 2 is an important difference between the two models.

- (3) Interpreting  $\mu < 0$  as a measure of instability, we conclude that, surprisingly, shorter columns are more unstable than taller ones. A typical dependence of  $\mu$  on  $H$  with  $\theta$  fixed is shown in Fig. 6(a). Note that the results obtained suggest that

$$\mu \rightarrow -\infty \quad \text{as} \quad H \rightarrow 0.$$

It was also observed that columns with small contact angles are more unstable than those with larger ones (see Fig. 6(b)), although  $\mu$  tends to a *finite* limit as  $\theta \rightarrow 0$ .

- (4) Examples of unstable perturbations  $f(z)$  are shown in Fig. 7. One can see that, in both cases,  $f$  has opposite signs for small and medium/large  $z$ . This suggests that the instability develops through self-amplifying exchange of liquid between the column's foot and its top/middle part.

- (5) We found it difficult to compute the solution of the eigenvalue problem for small  $\mu$  (for both models). This is due to the fact that, in the limit  $\mu \rightarrow 0$ , the small- $z$  behavior of  $f$  changes. This seemingly technical issue has important physical implications, which will be examined in Sec. V.

## V. NEUTRALLY STABLE COLUMNS

The case  $\mu = 0$  is particularly important for Model 2, where columns shorter than a certain threshold height are unstable. The simplest way to determine this threshold consists in setting  $\mu = 0$  and treating  $H$  as an unknown (the alternative eigenvalue).

It turns out, however, that this plan is not as straightforward as it appears.

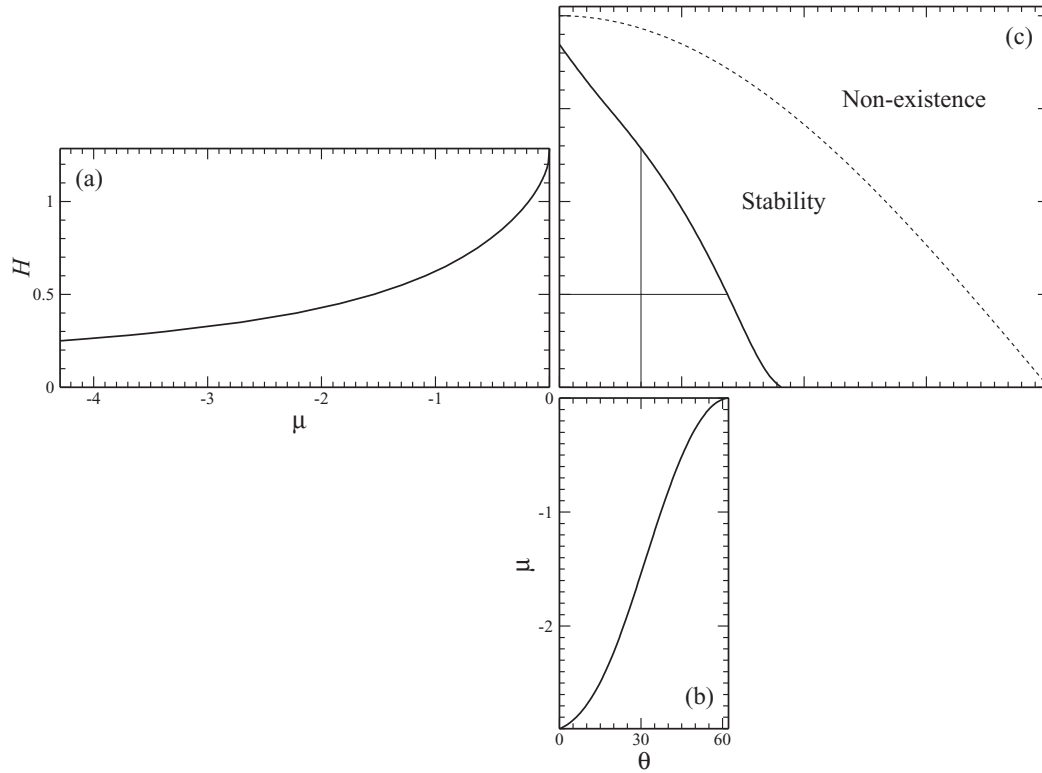


FIG. 6. The eigenvalue  $\mu$  vs. the columns' height  $H$  and the contact angle  $\theta$ , for Model 2.  $|\mu|$  reflects the strength of the instability. (a)  $\mu$  vs.  $H$  for  $\theta = 30^\circ$ . (b)  $\mu$  vs.  $\theta$  for  $H = 0.5$ . (c) The stability diagram for Model 2 (the same as in Fig. 5). Thin solid lines in panel (c) show the cross-sections corresponding to panels (a) and (b).

### A. Mathematical aspects of neutral stability

Letting  $\mu = 0$  in Eq. (34), taking the limit  $z \rightarrow 0$ , and recalling asymptotic (22), we obtain

$$-(z^3 \ln z f')' - \frac{zf}{\ln z} - \frac{\lambda \ln z}{2} = 0. \quad (37)$$

A particular solution for this equation can be chosen in the form

$$f_p \sim -\frac{\lambda}{2z} \quad \text{as } z \rightarrow 0, \quad (38)$$

whereas two linearly-independent solutions of the homogeneous version of Eq. (37) are obtained in Subsection B 2 of Appendix B,

$$f_1 \sim 1, \quad f_2 \sim \int \frac{dz}{z^3 \ln z} \quad \text{as } z \rightarrow 0. \quad (39)$$

Given (38) and (39), the general solution of (37) can be written in the form

$$f \sim -\frac{\lambda}{2z} + c_1 + c_2 \int \frac{dz}{z^3 \ln z} \quad \text{as } z \rightarrow 0, \quad (40)$$

where  $c_{1,2}$  are arbitrary constants. Evidently, the boundary condition (30) holds only if  $\lambda = c_2 = 0$ , so (40) reduces to

$$f \sim c_1 \quad \text{as } z \rightarrow 0. \quad (41)$$

Observe also that  $c_1$  plays the role of a normalizing constant – hence, it can only be used to satisfy the normalizing condition (29). As a result, we are left with only *one* unknown (the height  $H$  of the

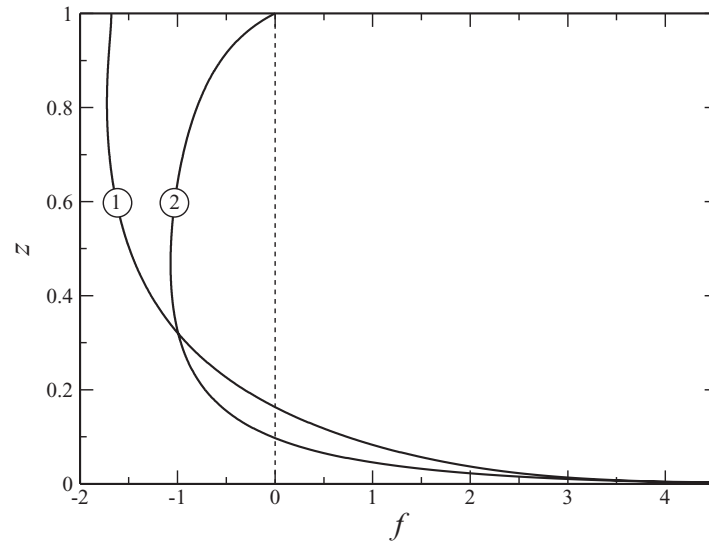


FIG. 7. The energy-minimizing perturbation  $f(z)$  for the column with  $H = 1$  and  $\theta = 30^\circ$ : (1) Model 1 (fixed contact angle), (2) Model 2 (fixed position of the contact line).

neutrally stable column) to satisfy *two* constraints (the volume-conserving condition (28) and the boundary condition at  $z = H$ ).

Thus, a solution exists for all negative  $\mu$  no matter how small  $|\mu|$  is – yet the problem appears to be over-determined in the limiting case  $\mu = 0$ .

To resolve the paradox, note that, even though  $\lambda$  – and, hence,  $f_p$  – vanishes as  $\mu \rightarrow 0$ , this does not necessarily mean that the contribution of  $f_p$  to the integral in (28) vanishes too. Given the singular nature of  $f_p$  in the double limit  $z, \mu \rightarrow 0$ , this contribution can tend to a *finite* value. In fact, it *must* tend to a finite value, as this is the only way to resolve the paradox. Accordingly, if the integral in (28) is calculated with the limiting contribution of  $f_p$  ignored, (28) does not hold.

The above argument suggests that, when dealing with neutral stability, the volume-preserving condition (28) can simply be omitted. Given that it holds for all finite values of  $\mu$ , one does not need to specifically enforce it for  $\mu = 0$ .

The physical meaning of this conclusion will be discussed later, whereas now we present the neutral stability curve for Model 2 computed *without* the volume-preserving condition (28) and compare it with curves for small but finite  $\mu$  computed *with* (28). The results are plotted on the  $(\theta, H)$ -plane in Fig. 8, which shows that, as  $\mu \rightarrow 0$ , the latter curves tend to the former.

This confirms that, in the limit of neutral stability, the volume-preserving condition (28) becomes unimportant.

## B. Physical aspects of neutral stability

Recall that, even though the pool of liquid in our problem is infinite, it was treated as a limit of increasingly large but finite pools. Accordingly, volume conservation was imposed, and unstable perturbations (i.e., those with  $\mu < 0$ ) were affected by this constraint. Yet, the neutrally stable case ( $\mu = 0$ ) has turned out to be independent of whether or not volume conservation is enforced. So far, this conclusion was obtained through mathematical means, but now it will be explained physically.

Consider an unstable perturbation, which reduces the energy of the column, but does *not* preserve the volume – i.e., the perturbation’s volume is, say, negative. We claim that, in this case, a modified perturbation can be constructed, such that satisfies the volume conservation with virtually no change to its energy.

To do so, one needs to elevate slightly the pool’s surface far away from the column. Provided the region of elevation is large enough, the “newly added” volume can cancel the negative volume of the

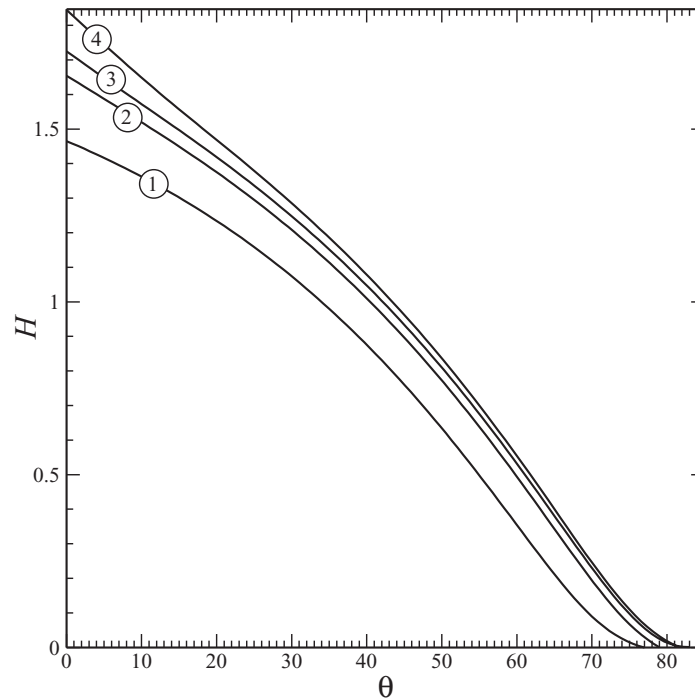


FIG. 8. Curves of equal  $\mu$  on the  $(\theta, H)$  plane, for Model 2: (1)  $\mu = -10^{-1}$ , (2)  $\mu = -10^{-2}$ , (3)  $\mu = -10^{-3}$ , (4)  $\mu = 0$ . Curve (4) is the same as that of neutral stability in Fig. 5.

original perturbation. At the same time, since the added volume is proportional to the elevation of the surface, whereas the added energy is proportional to the elevation *squared*, the latter is negligible and the perturbation remains unstable. One should keep in mind, however, that this argument holds only if the pool is infinite (otherwise the region where the surface needs to be elevated may not be large enough).

The fact that volume conservation does not affect neutral stability implies that this constraint cannot stabilize an otherwise unstable column, and vice versa. As a result, one can prove the instability of all columns in Model 1 in a much simpler way than how we did it above. One only needs to do so *without* constraint (28), and the results obtained will stand even if (28) is applied.

Indeed, omit the volume-conserving constraint (28) and observe that

$$f = \text{const.} \quad (42)$$

satisfies all of the remaining restrictions (29)–(31) of Model 1. At the same time, expression (27) for the energy's second variation yields  $\mathcal{E} < 0$ . Thus, all columns are unstable with respect to uniform contraction ( $f < 0$ ) or uniform widening ( $f > 0$ ), and this conclusion was obtained without solving any eigenvalue problems.

Note also that the above argument is inapplicable to Model 2, as perturbation (42) does not satisfy the boundary condition (32).

Finally, we emphasize that, even though the volume-preserving constraint (28) does not affect neutrally stable columns, it does affect the unstable ones. Accordingly, if one just needs to test a given column for stability, one can examine it without constraint (28). If, however, one wants to understand how instability occurs, volume preservation should certainly be assumed.

In particular, volume-preserving perturbations must change sign (as do those shown in Fig. 7). Physically this implies that instability develops through self-amplifying exchange of liquid between the foot of the column and its middle/top part.

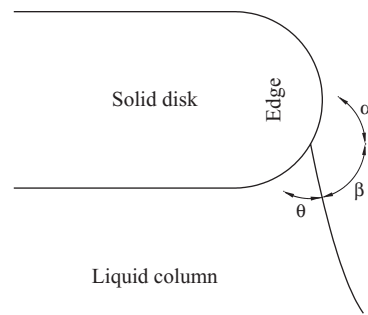


FIG. 9. A schematic illustrating a liquid column with its contact line located on the edge of the disk.

## VI. COMPARISON WITH THE RESULTS OF VOGEL, AND BENILOV AND ORON

The main conclusion of Ref. 1 is that, if the column's top does not cover the entire disk, the column is unstable. Given that the analysis of Ref. 1 was carried under Model 1, this conclusion agrees with our results.

Reference 1 also claimed that, if the column's top covers the entire disk, the contact line is pinned to the disk's edge. To understand why this is indeed the case, introduce the angle  $\alpha$  between the disk's surface and the horizontal, and the angle  $\beta$  between the *column's* surface and the horizontal (see Fig. 9). Then, if a Model-1 column retreats from the disk's edge,  $\alpha$  can change by up to  $180^\circ$  (depending on where it was originally) – and so can  $\beta$  (because  $\beta = 180^\circ - \theta - \alpha$  with  $\theta = \text{const.}$ ). As a result, the column can significantly change its shape (since that depends on  $\beta$ ).

Let us now consider the limit of an infinitely thin disk. In this case, an *infinitesimal* retreat of the contact line from the disk's edge implies a *finite* change in its shape (and, therefore, energy). Clearly, this kind of disturbance cannot be treated as small and, thus, should be disallowed in a linear stability study.

Thus, the cases where the column's top covers the entire disk should be treated under Model 2 (pinned contact line), and our results suggest that such columns can be stable (which agrees with the hypothesis of Ref. 1). Finally, note that Ref. 1 did not examine Model-2 columns with their tops *not* covering the entire disk.

Reference 2, in turn, examined the stability of Model-1 columns with respect to a particular class of disturbances and found that sufficiently low columns are unstable. It was also shown that, if the set of allowable disturbances is expanded, so does the region of instability. In the light of the present findings, we can add that further expansions of the set of allowable disturbances would eventually make *all* Model-1 columns unstable.

## VII. SUMMARY AND CONCLUDING REMARKS

Thus, we have examined the stability of a liquid column rising from an infinite pool, with its top attached to a horizontal plate suspended at a certain height above the pool's surface. Two different models have been used for the column's contact line: Model 1 assumes the contact angle to always equal Young's equilibrium value, and Model 2 assumes a functional dependence between the contact angle and the velocity of the contact line. It was further assumed that this dependence involves a hysteresis interval, and it was argued (Sec. II C) that, in this case, the contact line is pinned to the plate.

It has been demonstrated that, in Model 1, all liquid columns are unstable – whereas, in Model 2, both unstable and stable columns exist. This proves that pinning of the contact line (as in Model 2) is a stabilizing effect. The stability diagram on the  $(\theta, H)$ -plane has been computed for Model 2 (see Fig. 5).

For both models, the most unstable perturbation is radially symmetric, and instability occurs (if it does) due to self-amplifying exchange of liquid between the foot of the column and its middle/top part.

Finally, we shall make two comments of general nature:

1. In this work, we dealt only with those perturbations that preserve volume, but it turned out that this constraint does *not* affect the case of neutral stability. Thus, if one needs to find out if a given column is stable, the constraint of volume preservation does not have to be imposed. It should only be used to determine the shape of the most unstable disturbance for unstable columns. This conclusion is likely to apply to all capillary surfaces in unbounded domains.
2. The stability of liquid columns is the second problem where the hysteresis of the contact-line law is linked to pinning of contact lines (the first one was the stability of rivulets examined in Ref. 3). It appears that such a model may be useful for further studies of stability of capillary surfaces and flows.

In conclusion, it is interesting to speculate what happens with a stable (Model-2) column if the disk to which it is attached is slowly lifted up. It turns out that the evolution in this case is best explained using the dependence of the radius  $R$  of the top of the column on its height  $H$  shown in Fig. 4.

When  $H$  begins to grow, the column's contact line remains stationary as long as  $\theta$  stays inside the hysteresis interval. Thus,  $R$  remains fixed while  $H$  is increasing – in terms of Fig. 4, this implies that the solution is moving along a horizontal line going from left to right – i.e., from larger to smaller values of  $\theta$ . Eventually,  $\theta$  reaches the lower boundary of the hysteresis interval  $\theta_r$ , after which the contact line has to recede, i.e.,  $R$  has to decrease.

Next, assume that the disk is lifted slowly enough, so that  $\theta$  stays close to  $\theta_r$ . In this case, any possible scenario of further evolution implies that

- $\theta$  remains constant.
- $H$  increases, while  $R$  decreases.

These two requirements, however, are impossible to combine. Indeed, if  $\theta$  is to remain constant,  $H$  and  $R$  must either *both* increase or *both* decrease (see Fig. 4). This effectively means that, once  $\theta$  has reached  $\theta_r$ , no steady solution exists for the column to evolve to – and the only possible scenario in this case is the column's breakdown.

Thus, we conclude that the factor limiting the height of a liquid column is the non-existence of a steady solution with suitable parameters (which agrees with the conjecture made in Ref. 2).

## ACKNOWLEDGMENTS

The authors acknowledge the support of the Science Foundation Ireland under Grant Nos. 11/RFP.1/MTH3281 and 12/IA/1683. We are also grateful to Dr. S. Belochapkin who helped us with the experimental part of this work.

## APPENDIX A: PROPERTIES OF EQ. (34)

Before solving Eq. (34) numerically, we need to clarify the behavior of its solutions near the singular point  $z = 0$ .

Letting in Eq. (34)  $z \rightarrow 0$  and taking into account asymptotics (18), we obtain<sup>13</sup>

$$-\left[\frac{r}{(r')^3}f'\right]' - \frac{f}{rr'} + \frac{\lambda r}{2} + \mu f = 0 \quad \text{as } z \rightarrow 0. \quad (\text{A1})$$

We shall represent the general solution of (A1) in the form

$$f = c_1 f_1 + c_2 f_2 + f_p, \quad (\text{A2})$$

where  $f_{1,2}$  are two linearly independent solutions of the homogeneous version of Eq. (A1) (i.e., that with  $\lambda = 0$ ),  $f_p$  is a particular solution of the full equation, and  $c_{1,2}$  are arbitrary constants.  $f_p$  can be

found asymptotically by assuming that the first two terms in Eq. (A1) are much smaller than the last two. Equating the latter, we obtain

$$f_p \sim -\frac{\lambda r}{2\mu} \quad \text{as } z \rightarrow 0. \quad (\text{A3})$$

This solution can now be used to verify that the first two terms in Eq. (A1) are indeed negligible.

$f_{1,2}$ , in turn, depend strongly on the sign of  $\mu$ .

(1) If  $\mu < 0$ ,  $f_{1,2}$  can be found through an asymptotic method (see Subsection B 1 of Appendix B) similar to that of Wentzel-Kramers-Brillouin (WKB),

$$f_1 \sim \frac{(-r')^{3/4}}{r^{1/4}} \exp \left[ \int \sqrt{\frac{\mu (r')^3}{r}} dz \right] \quad \text{as } z \rightarrow 0, \quad (\text{A4})$$

$$f_2 \sim \frac{(-r')^{3/4}}{r^{1/4}} \exp \left[ - \int \sqrt{\frac{\mu (r')^3}{r}} dz \right] \quad \text{as } z \rightarrow 0. \quad (\text{A5})$$

Recalling asymptotics (22), and also that  $\mu < 0$ , one can see that  $f_1$  grows exponentially as  $z \rightarrow 0$  – hence, the boundary condition (30) holds only if

$$c_1 = 0. \quad (\text{A6})$$

The remaining constant  $c_2$ , together with  $\lambda$  and  $\mu$ , are sufficient to satisfy the two integral conditions (28) and (29) and the boundary condition at  $z = H$ .

(2) If  $\mu > 0$ , (A4) and (A5) are to be replaced with

$$f_1 \sim \frac{(-r')^{3/4}}{r^{1/4}} \sin \left[ \int \sqrt{-\frac{\mu (r')^3}{r}} dz \right] \quad \text{as } z \rightarrow 0,$$

$$f_2 \sim \frac{(-r')^{3/4}}{r^{1/4}} \cos \left[ \int \sqrt{-\frac{\mu (r')^3}{r}} dz \right] \quad \text{as } z \rightarrow 0.$$

Even though both  $f_{1,2}$  satisfy the boundary condition (30), they are meaningless physically (as they oscillate at an increasing rate as  $z \rightarrow 0$ , i.e., far away from the column). We shall not discuss  $f_{1,2}$  in further detail, as the case  $\mu > 0$  is complementary to the (simpler) case  $\mu < 0$ .

In other words, one only needs to determine which columns are unstable, as all the remaining ones are inevitably stable.

## APPENDIX B: THE WKB METHOD FOR THE HOMOGENEOUS VERSION OF EQ. (A1)

### 1. The case $\mu \neq 0$

Consider the homogeneous version of (A1),

$$-\left[ \frac{r}{(r')^3} f' \right]' - \frac{f}{rr'} + \mu f = 0, \quad (\text{B1})$$

where  $z$  is implied to be small. Assuming

$$z \sim \varepsilon, \quad \frac{d}{dz} \sim \frac{1}{\varepsilon}, \quad (\text{B2})$$

where  $\varepsilon$  is a small parameter, and taking into account asymptotic (22), one can estimate the terms of Eq. (B1),

$$\left[ \frac{r}{(r')^3} f' \right]' \sim \varepsilon \ln \varepsilon, \quad \frac{f}{rr'} \sim \frac{\varepsilon}{\ln \varepsilon}, \quad \mu f \sim 1. \quad (\text{B3})$$



Thus, there is an implicit small parameter in front of the highest derivative in Eq. (B1), which suggests that it can be solved asymptotically using a WKB-style approach.

In principle, we could use (B2) to re-scale Eq. (B1), but the presence of logarithmic terms makes the formal expansion awkward. It is more convenient to introduce  $F$  such that

$$f = e^F, \quad (\text{B4})$$

for which (B1) yields

$$F'' + \left( \frac{r'}{r} - \frac{3r''}{r'} \right) F' + (F')^2 = \mu \frac{(r')^3}{r} - \frac{(r')^2}{r^2}.$$

We assume that  $|F|$  is large (which can be verified *a posteriori*) – hence,

$$(F')^2 \gg |F''| \sim \left| \left( \frac{r'}{r} - \frac{3r''}{r'} \right) F' \right|. \quad (\text{B5})$$

Next, using asymptotic (22), it can be shown, that for small  $z$ :

$$\left| \mu \frac{(r')^3}{r} \right| \gg \left| \frac{(r')^2}{r^2} \right|.$$

Then, seeking the solution in the form

$$F = F_0 + F_1 + \dots, \quad (\text{B6})$$

we assume  $F_0$  and  $F_1$  to satisfy

$$(F_0')^2 = \mu \frac{(r')^3}{r},$$

$$F_0'' + \left( \frac{r'}{r} - \frac{3r''}{r'} \right) F_0' + 2F_0'F_1' = -\frac{(r')^2}{r^2},$$

which yield

$$F_0' = \pm \left[ \frac{\mu (r')^3}{r} \right]^{1/2}, \quad (\text{B7})$$

$$F_1' = \mp \frac{1}{2} \left[ \frac{r'}{\mu r^3} \right]^{1/2} - \frac{1}{4} \left( \frac{r'}{r} - \frac{3r''}{r'} \right). \quad (\text{B8})$$

Using asymptotic (22), one can show that the first term on the right-hand side of (B8) is much smaller than the second term, and omitting the former, we obtain

$$F_1 = -\frac{1}{4} (\ln r - 3 \ln r'). \quad (\text{B9})$$

The asymptotic expressions (A4) and (A5) in the main body of the paper follow from (B4), (B6)–(B7), and (B9). The solution found can also be used to verify our original assumption (B5).

## 2. The case $\mu = 0$

Omitting the non-homogenous term (involving  $\lambda$ ) from Eq. (37), we obtain

$$-(z^3 \ln z f')' - \frac{zf}{\ln z} = 0, \quad (\text{B10})$$

where  $z$  is implied to be small, so estimates (B3) still apply. This time, they indicate that the first term in Eq. (B10) is much larger than the second term. Omitting the latter, we obtain

$$-(z^3 \ln z f')' = 0,$$

which yields

$$f = c_1 + c_2 \int \frac{dz}{z^3 \ln z}. \quad (\text{B11})$$

This solution corresponds to (39) of the main body of the paper.

## APPENDIX C: THE NUMERICAL ALGORITHMS USED

In this appendix, we shall describe the numerical algorithms used for the eigenvalue problems (34), (28)–(31) (Model 1) and (34), (28)–(30), (32) (Model 2). In both cases, the function  $r(z)$  is supposed to have already been computed using Eqs. (17)–(19) (Model 1) or (17)–(18), (20) (Model 2) (for more details, see Ref. 2).

### 1. The case $\mu \neq 0$

In all cases considered it turned out that, if  $\mu \neq 0$ , then  $\lambda \neq 0$  – hence, in principle,  $\lambda$  can be eliminated through substitution (35). It is more convenient, however, to omit the normalizing condition (29) altogether and normalize  $f$  by setting

$$\lambda = -2\mu, \quad (\text{C1})$$

in which case asymptotics (A2)–(A6) yield

$$f \sim c_2 \frac{(-r')^{3/4}}{r^{1/4}} \exp \left[ - \int \sqrt{\frac{\mu (r')^3}{r}} dz \right] + r \quad \text{as } z \rightarrow 0. \quad (\text{C2})$$

Observe that the first term in (C2) decays exponentially as  $z \rightarrow 0$ , so  $f$  is dominated by the (logarithmically growing) second term. Thus, when solving the problem numerically, we replaced (C2) by the following approximate boundary condition:

$$f \approx r \quad \text{at } z = z_0, \quad (\text{C3})$$

where  $z_0 \ll 1$ . Then, for a given  $\mu$ , Eq. (34) was discretized using central differences for the derivatives and solved together with the boundary conditions (31) and (C3) (for Model 1) or (32) and (C3) (for Model 2), as a set of linear non-homogeneous equations. Once  $f(z)$  had been found, the left-hand side of the volume-preserving condition (28) was computed and fed into a root finding routine based on the secant method. This routine would yield the value of  $\mu$  for which the left-hand side of (28) was indeed zero.

### 2. The case $\mu = 0$ , Model 2

This case is governed by Eq. (34) with  $\mu = \lambda = 0$ , the normalizing condition (29), and the boundary conditions (32) and (41). The parameter  $H$  is to be treated as an unknown.

The shooting method was employed. Using asymptotic (41) with, say,  $c_1 = 1$  the solution was “shot” from  $z = 0$  toward  $z = H$ . The resulting value of  $f(H)$  was fed into a root finding routine based on the secant method which would find  $H$  for which  $f(H) = 0$ , so the boundary condition (32) holds.

Finally, the normalizing condition could be enforced by multiplying the solution for  $c_1 = 1$  by a suitable constant.

<sup>1</sup> T. I. Vogel, “Symmetric unbounded liquid bridges,” *Pac. J. Math.* **103**, 205 (1982).

<sup>2</sup> E. S. Benilov and A. Oron, “The height of a static liquid column pulled out of an infinite pool,” *Phys. Fluids* **22**, 102101 (2010).

<sup>3</sup> E. S. Benilov, “On the stability of shallow rivulets,” *J. Fluid Mech.* **636**, 455 (2009).

<sup>4</sup> I. M. Gelfand and S. V. Fomin, *Calculus of Variations* (Prentice-Hall, Englewood Cliffs, NJ, 1963).

<sup>5</sup> V. I. Arnold, “Conditions for nonlinear stability of stationary plane curvilinear flows of an ideal fluid,” *Sov. Math. Dokl.* **162**, 773 (1965) [*Dokl. Akad. Nauk SSSR* **162**, 975 (1965)].

<sup>6</sup> M. Giaquinta and S. Hildebrandt, *Calculus of Variations* (Springer, Berlin, 1996), Vol. 1.

<sup>7</sup> L. M. Hocking, “Sliding and spreading of thin two-dimensional drops,” *Q. J. Mech. Appl. Math.* **34**, 37 (1981).

<sup>8</sup> H. P. Greenspan, “On the motion of a small viscous droplet that wets the surface,” *J. Fluid Mech.* **84**, 125 (1978).

<sup>9</sup> R. Finn, *Equilibrium Capillary Surfaces* (Springer, New York, 1986).

<sup>10</sup> P.-G. de Gennes, F. Brochard-Wyart, and D. Quere, *Capillarity and Wetting Phenomena: Drops, Bubbles, Pearls, Waves* (Springer, New York, 2003).

<sup>11</sup> D. Langbein, *Capillary Surfaces: Shape – Stability – Dynamics, in Particular Under Weightlessness* (Springer, Berlin, 2002).

<sup>12</sup> The method for computing the neutral stability curve in Fig. 5 is discussed in Sec. V.

<sup>13</sup> Given the asymptotic nature of Eq. (A1), we could have replaced in it  $r$  with its asymptotic (22). However, in view of the relatively low accuracy of (22), it is better to leave  $r$  as is.